

MODELING AND FAILURE CONTROL OF SPACECRAFT PRESSURIZED STRUCTURES SUBJECT TO ORBITAL DEBRIS IMPACT

Frederick Cook*, Igor Telichev**

*University of Manitoba, Department of Mechanical and Manufacturing Engineering
E2-327 EITC, 75A Chancellors Circle 2500 Winnipeg, Manitoba, Canada R3T 5V6
(*Email: umcook4@cc.umanitoba.ca; (**Email: igor.telichev@ad.umanitoba.ca)*

ABSTRACT

Motivated by the dramatic worsening and uncertainty of orbital debris situation, the present paper is focused on the structural integrity of the spacecraft pressurized modules/pressure vessels. The objective is to develop a methodology of numerical simulation of the spacecraft pressurized structure behaviour under hypervelocity impact, including simulation of the following processes: a) formation of the impact damage of the pressure wall; b) loading and failure of structure. The analysis was performed by the method of singular integral equations

1. INTRODUCTION

The series of incidents happened in last six years demonstrated that only one or two collisions can drastically change the orbital debris population. With space activity continuously running and expanding, the rate of collisions in space also increases, leading in turn to a new reality for the orbital debris environment where all functioning spacecraft are under higher risk than they were designed for. This is a particular concern for the case of both shield and pressurized wall perforation which presents a potential for the pressure wall failure in an abrupt fashion [1-4]. The answer to the question whether the spacecraft pressurized structure would undergo “unzipping” due to the impact of undetectable debris is crucial for the mission success or failure. Essentially, it quantifies not only the spacecraft survivability but on the first place the compliance with the applicable post mission disposal requirements.

Nowadays, the pressurized modules and high pressure tanks of the most heavily shielded spacecrafts are able to withstand the impact of debris up to one centimeter in diameter. The orbital debris between 1 and 5-10 cm in size which is too small to be tracked but large enough to cause the shielded pressure wall perforation, poses the

highest risk for the spacecraft mission. The 5 cm dimension represents the lowest border for the ground-base instrumentation sensitivity currently available for the objects tracking.

Fig. 1 illustrates the survivability-driven design logic where it is assumed that impact of undetectable debris between 1 and 5-10 cm in size has occurred and the pressure wall is damaged. This design concept requires that when developing spacecraft, all attempts be made to prevent the accidental spacecraft breakups. The mitigation and protection measures are assessed for effectiveness through the fracture analysis (Fig. 1, module 5). In the event that a pressure wall is predicted to “unzip”, the survivability improvements can be achieved by adding more effective shielding or/and by varying the design parameters of the pressurized module. New protection measures will be evaluated by repeating the steps in the above design procedure (Fig. 1) until the “no rupture” conditions will be verified. The analysis of interaction of penetrative particles with equipment inside a spacecraft is out of scope of the current paper.

This methodology is viewed as a key element in the survivability-driven spacecraft design procedure providing that under no circumstances will the “unzipping” occur if the particle dimension does not exceed the specified value, e. g. 10 mm. Addressing this problem will not only improve the survivability of spacecraft itself but also will provide the mitigation effect since each satellite break-up causes not only the loss of space assets but the considerable addition to the orbital debris population.

2. MODELING OF IMPACT DAMAGE

Experimental studies have shown that the impact damage has the form of a hole surrounded by a zone of

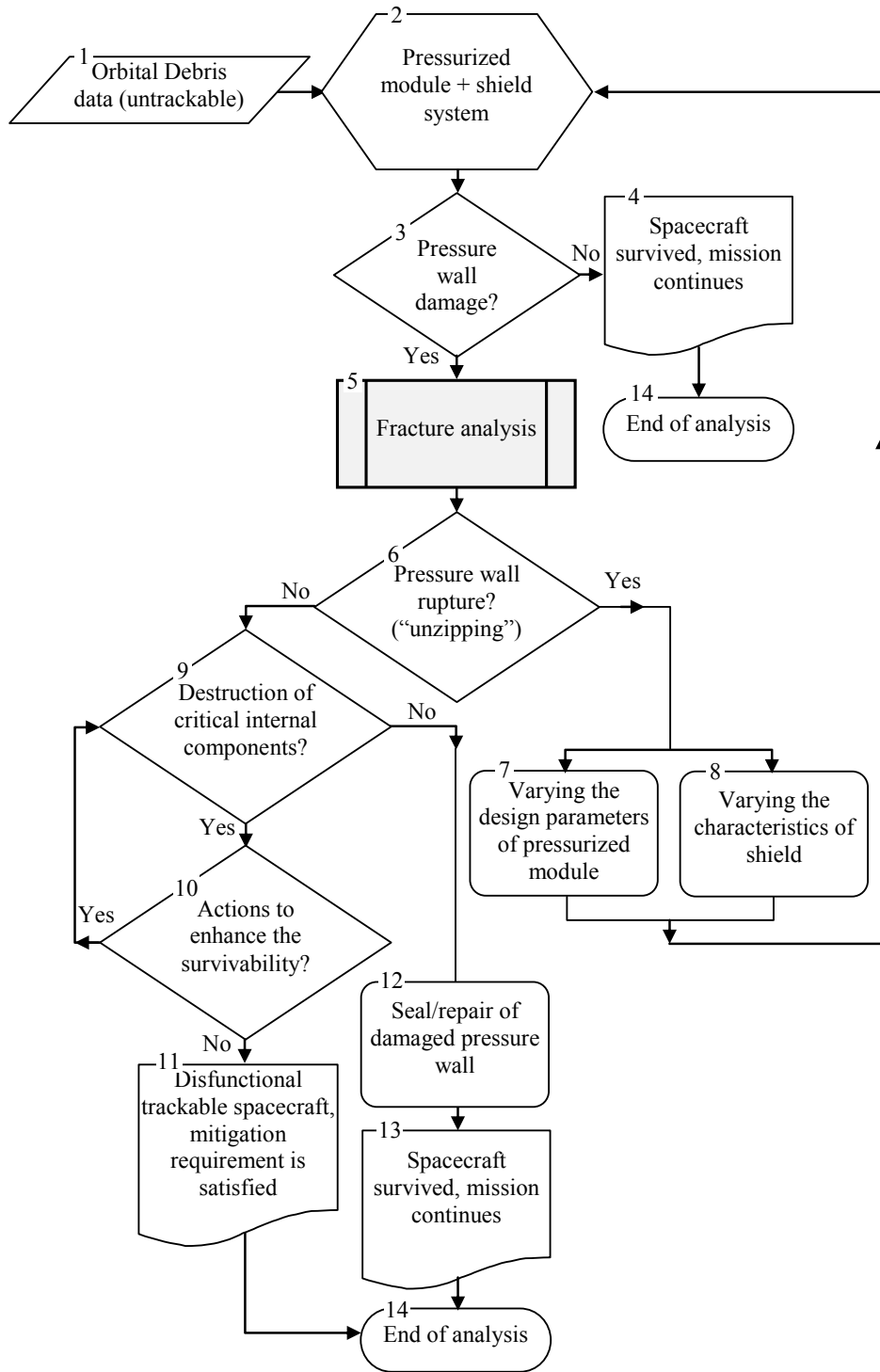


Figure 1. Design procedure of spacecraft with enhanced survivability

the crack-like defects (Fig. 2a, b, c). For the case of both shield and pressure wall perforation the impact damage varies from the petal hole (Fig. 2a) to the “cookie-cutter hole” (Fig. 2b). The perforation of the unshielded wall is

accompanied by a zone of spall cracks adjacent to the impact hole as shown in Fig. 2c. For further analysis it suggested to model the cracked area around the penetrated hole by two radial cracks emanating from the

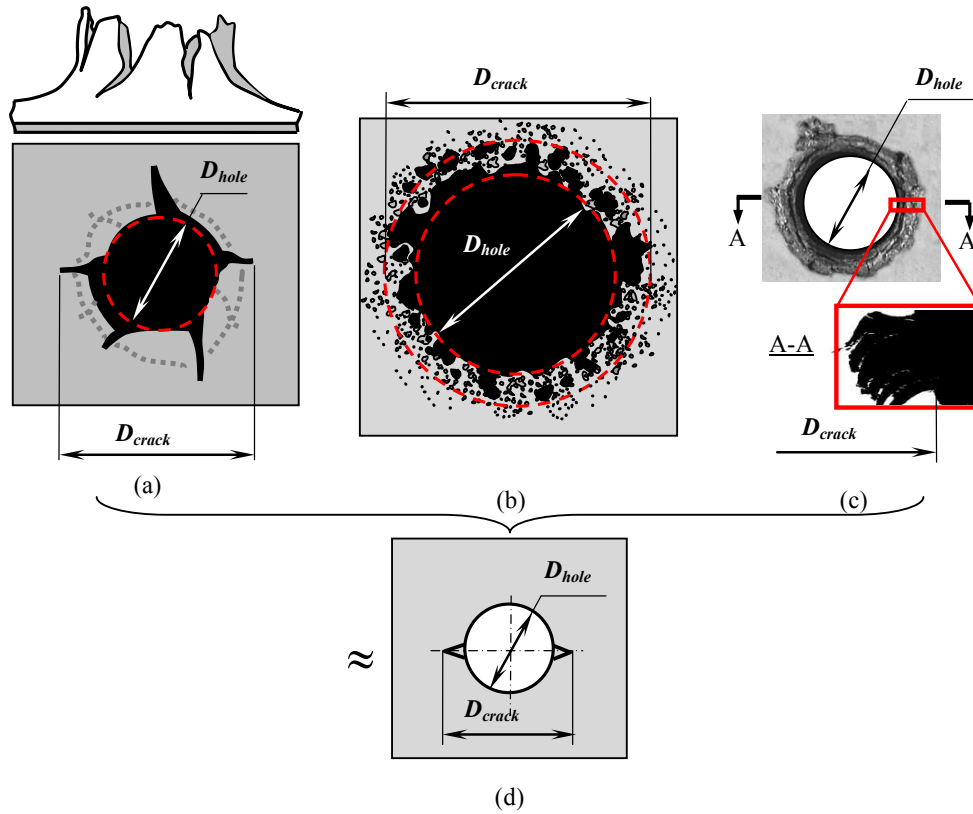


Figure 2. Modeling the impact holes: a) petal hole; b) “cookie-cutter hole”; c) hole with adjacent spall cracks; d) model of impact hole

rim of the hole perpendicularly to the applied load. The diameter of the model hole is equal to the diameter of the impact hole (D_{hole}), while the length of the fictitious radial cracks is bounded by a damage zone (D_{crack}). In cylindrical pressurized structure these two radial cracks are set to be normal to the hoop stress, i.e. along the expected fracture path (Fig. 2d).

3. MODELING OF FRACTURE

3.1 Solution of Singular Integral Equation

The problem of potential fracture and bursting of aerospace pressurized structures was extensively examined by the NASA Advanced Fracture Mechanics Group [1-3]. The fracture propagation analysis was conducted analytically using the linear elastic fracture mechanics approach and numerically employing the finite element method and non-linear fracture mechanics technique. Comparison to the experimental data showed that the linear elastic fracture mechanics methods are too conservative and non-linear fracture mechanics approach is required for a more realistic treatment of the problem [1].

We assumed that a single hole with two radial cracks is

located in the infinite plate made of an isotropic elastic perfectly plastic material, the zones of plasticity are localized along the crack prolongations and the compressive stresses within the plastic zones σ_{pz} are equal to the tensile yield limit σ_y . The evolution of the stress field near the perforated hole can be evaluated explicitly using the Autodyn® code (Fig. 3).

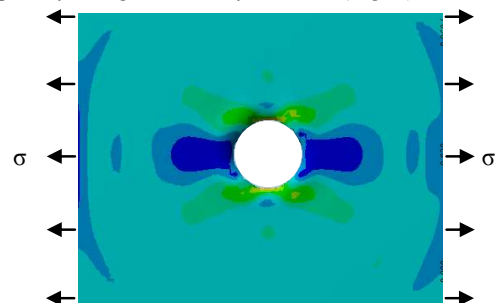


Fig. 3. Snapshot of the evolution of the stress field after the hole was instantly formed in the loaded plate

The problem can be formulated in terms of a singular integral equation (SIE). The singular integral equation technique is a powerful alternative to the finite element method in the non-linear

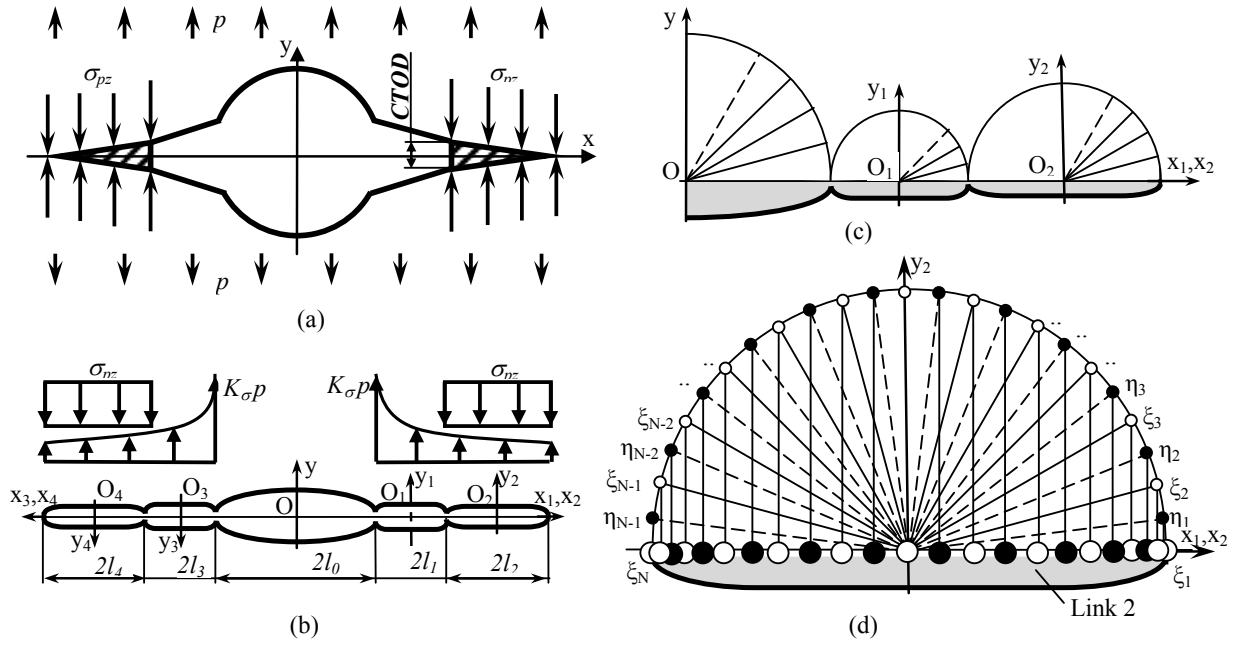


Figure 4. 5-link crack (a, b) and Chebyshev's nodes on the crack face(c, d)

analysis of crack propagation which provides very rapid convergence of the numerical results [5]. The solution of the singular integral equation (1) includes the following basic steps.

Step 1: The analysis starts with specifying the design and material characteristics of the pressure wall and determining the impact hole parameters.

Step 2: The piecewise traction distribution is applied to the crack surface as it shown in Fig. 4a, b. It divides the contour into 5 portions (links) where each piece of the traction function is differentiable throughout each individual link. The traction-free link L_0 corresponds to the hole, links L_1 and L_3 are radial cracks and links L_2 and L_4 represent the plastic zones. The solution of the singular integral equation must satisfy the condition of single-valuedness of displacements for the crack contour. Also, the symmetry of the problem and link angular positions are taken into account.

Step 3: Unlike the finite element method the method of singular integral equations is free of mesh generation and only nodes are needed. The Chebyshev's nodes with normalized coordinates ξ and η changing from -1 to 1 are generated on each link of the contour (Fig. 4 c, d). The open circles indicate the points ξ_1, \dots, ξ_N on the crack faces where displacements are calculated. The closed circles correspond to the traction nodes $\eta_1, \dots, \eta_{N-1}$. The normalized coordinates ξ and η change from -1 to 1.

Step 4: An efficient approach to account for the jump discontinuities of traction applied to the crack faces was proposed by Savruk [5]. Following [5] the single SIE for the case of 5-link crack is replaced by the system of singular integral equations. Also, the symmetry of the

problem and link angular positions are taken into account.

Step 5: The numerical solution of the system of singular integral equations is obtained by the method of mechanical quadratures [5]. By applying the Gauss-Chebyshev quadrature expressions the system of singular integral equations is transformed to the closed system of linear algebraic equations with $3N$ unknowns where N is number of the Chebyshev nodes.

Step 6: Once a solution of such system of equations is obtained, the stress intensity factor (SIF) at the end of the plastic strip can be evaluated.

Step 7: The unknown length of the plastic zones is determined from the condition that the stress intensity factor is equal to zero at the end of the plastic strip. The search is performed by golden section method.

Step 8: Using the expansion in terms of Lagrange interpolation polynomials over the Chebyshev nodes the crack opening profile for the entire crack (Fig. 5) and the opening displacement (CTOD) specifically at the crack tip can be calculated. It allows calculating the crack tip opening angle as well. The developed numerical algorithm provides the convergence for calculating the CTOD value up to a high level of loading (Fig. 6).

Step 9: The critical crack tip opening displacement is used as a fracture criterion. The problem to be solved involves the definition of the unknown plastic zones size and CTOD to determine if there is a case of simple perforation without crack growth from the impact hole or crack propagation and subsequently catastrophic rupture.

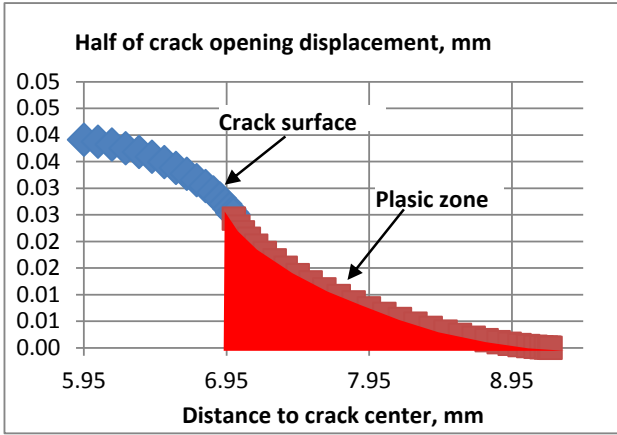


Fig. 5. Crack profile

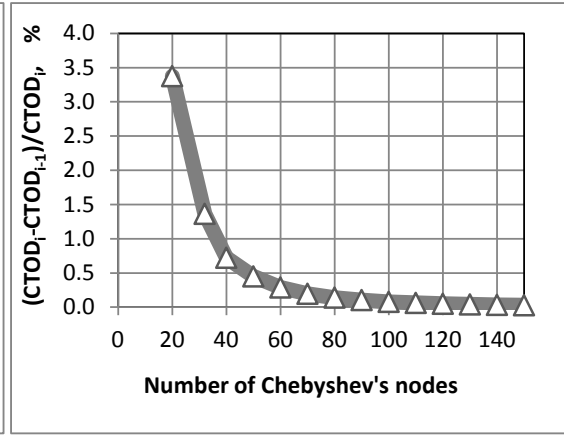


Fig. 6. Convergence of CTOD calculation

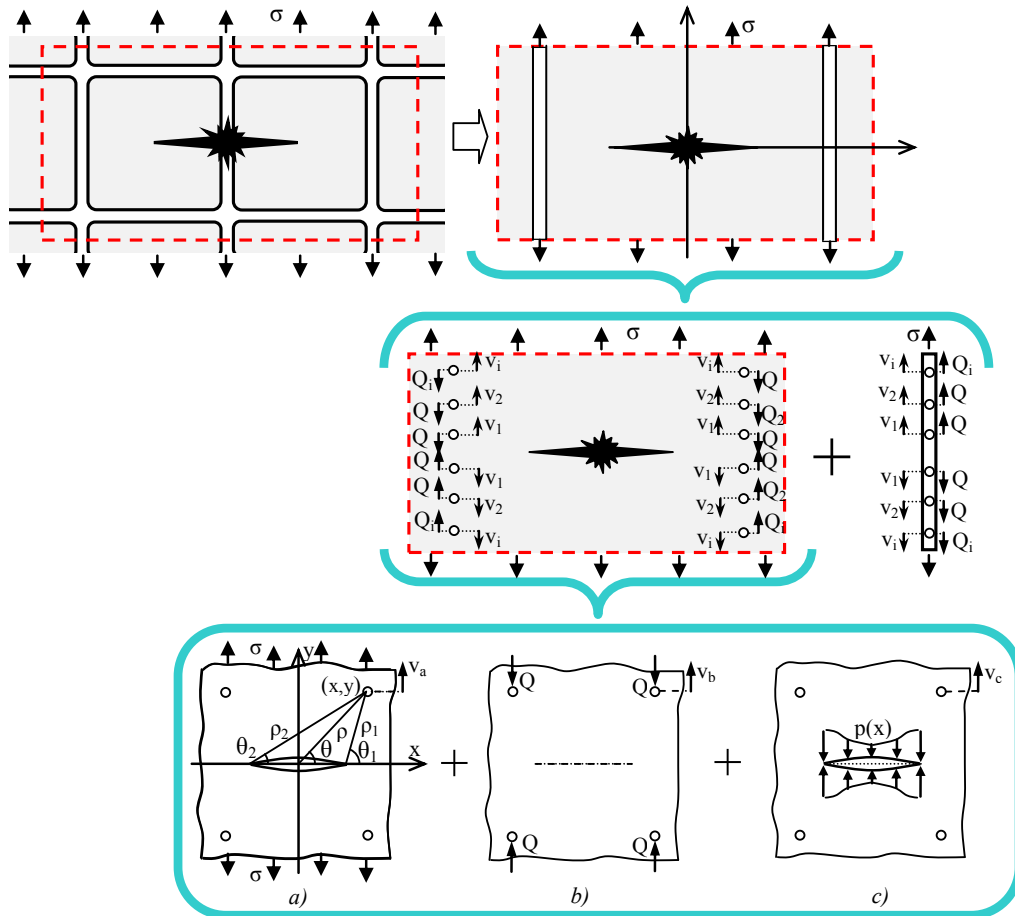


Fig. 7. Forces acting on stiffeners and skin

3.2 Effect of the stiffening elements

The stiffening elements in the reinforced thin-walled pressurized structures can be extremely effective in reducing the CTOD/CTOA, resulting in the crack arrest. The case of impact damage with completely broken central stiffener (Fig. 7) is considered as most severe scenario.

Owing to the presence of the crack, the load will be transferred from the pressure wall to the stiffener. Meanwhile the stiffener will exert the equivalent reaction forces on the pressure wall. For the analysis purpose the continuous load distribution is replaced by a set of the forces Q_1, Q_2 , etc. (Fig. 7) corresponding to a series of discrete segments of the skin-stiffener interface. These forces act in opposite directions on the pressure wall and stiffener.

The effect of such forces on the crack propagation behaviour is implemented by the displacement compatibility method outlined in [7, 8]. This method is based on the concept that displacements in the cracked panel should be equal to the corresponding displacements in the stiffeners. To determine the displacements in the pressure wall and stiffener at the centres of the discrete segments the stiffened structure is split up into its components (Fig. 7). The problem can be reduced to the superposition of uniformly loaded cracked plate, a plate without a crack, loaded with forces Q_1, Q_2 , etc and a cracked plate with traction on the crack faces [7, 8].

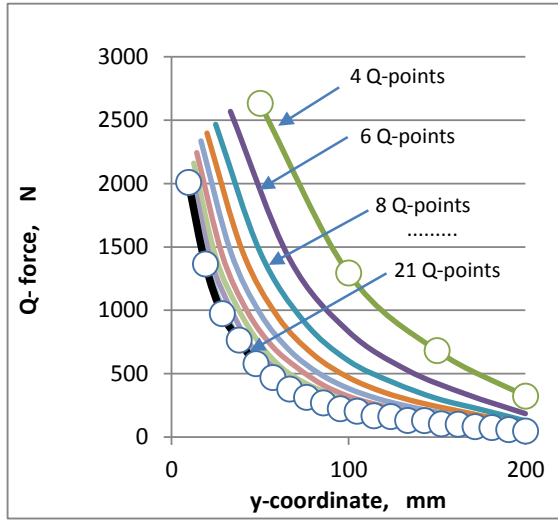


Fig.8. Convergence of Q -force calculation

The displacement at the i -th segment center (v_i) in the pressure wall and stiffener (v_i^s) can be expressed as following

$$v_i = \sum_{j=1} A_{ij} Q_j + B_i S \quad (1)$$

$$v_i^s = \sum_{j=1} A_{ij}^s Q_j + B_i^s S \quad (2)$$

where A_{ij}, A_{ij}^s, B_i and B_i^s are influence coefficients; indices i and j refer to the points in only one quadrant of the pressure wall. The coefficients A_{ij} and A_{ij}^s represent the displacements in the cracked shell and stiffener at the i -th point because of unit values of Q_j , while B_i and B_i^s coefficients represent the equivalent displacements because of unit values of σ . The condition of the equal displacements (v_i) and (v_i^s) gives the equation (3):

$$\sum_{j=1} (A_{ij} + A_{ij}^s) Q_j - (B_i - B_i^s) \sigma = 0 \quad (i=1, 2, \dots) \quad (3)$$

The influence coefficients B_i can be determined from the equation of displacement of the point (x, y) of the cracked sheet due to the uniaxial stresses σ (Fig 7a) [9] by setting the stress σ equal to unity:

$$v = \frac{\sigma}{E} \sqrt{\rho_1 \rho_2} \left[2 \sin \left(\frac{\theta_1 + \theta_2}{2} \right) - \frac{(1 + \nu) y \rho}{\rho_1 \rho_2} \cos \left(\theta - \frac{\theta_1 + \theta_2}{2} \right) \right] + v \frac{\sigma}{E} y \quad (4)$$

where E is Young's modulus of elasticity; ν is Poisson's ratio; a is the half-crack length.

$$\begin{aligned} \text{Here } \rho &= \sqrt{x^2 + y^2}; & \rho_1 &= \sqrt{(x-a)^2 + y^2}; \\ \rho_2 &= \sqrt{(x+a)^2 + y^2}; & \theta &= \arctan \left(\frac{y}{x-a} \right), \\ \theta_1 &= \arctan \left(\frac{y}{x-a} \right); & \theta_2 &= \arctan \left(\frac{y}{x+a} \right), \end{aligned}$$

The influence coefficients B_i^s are determined from the expression for the y -component of the stiffener displacement $v = \sigma/E$ by setting σ equal to unity.

The displacement for a cracked plate with symmetrically applied point forces (Fig. 7b, c) can be obtained from [Ref.] as following

$$v = \frac{(1+\nu)Q}{16\pi t E} \left[(3-\nu)\Omega + \frac{8y}{\pi} \int_0^a (\Delta \Gamma) d\xi \right] \quad (5)$$

where t is the pressure wall thickness; w is the stiffener width. The equation (5) will be used for calculation of the influence coefficients A_{ij} by setting Q equal to unity applied at (x_0, y_0) .

Here

$$\begin{aligned} \Omega &= (\alpha_1 + 1) \ln \left[\frac{(\alpha_1 + 1)^2 + \alpha_4^2}{(\alpha_1 + 1)^2 + \alpha_2^2} \right] - (\alpha_2 - 1) \ln \left[\frac{(\alpha_1 - 1)^2 + \alpha_4^2}{(\alpha_1 - 1)^2 + \alpha_2^2} \right] + \\ &4 \left(\frac{1-\nu}{3-\nu} \right) \left\{ \alpha_4 \left[\arctan \left(\frac{2\alpha_4}{\alpha_1^2 + \alpha_4^2 - 1} \right) + \arctan \left(\frac{2\alpha_4}{\alpha_2^2 + \alpha_4^2 - 1} \right) \right] - \right. \\ &\left. \alpha_3 \arctan 2\alpha_3\alpha_1 2 + \alpha_3 2 - 1 + \arctan 2\alpha_3\alpha_2 2 + \alpha_3 2 - 1; \right. \end{aligned}$$

$$\alpha_1 = \frac{2(x-x_0)}{w}; \quad \alpha_2 = \frac{2(x+x_0)}{w}; \quad \alpha_3 = \frac{2(y-y_0)}{w}; \quad \alpha_4 = \frac{2(y+y_0)}{w};$$

$$\begin{aligned} \Lambda &= \ln \left(\frac{a^2 - \xi^2 + 2\sqrt{a^2 - \xi^2} \sqrt{C_1 + C_2 + 2C_2}}{a^2 - \xi^2 - 2\sqrt{a^2 - \xi^2} \sqrt{C_1 + C_2 + 2C_2}} \right) \\ &- \frac{(1+\nu)y\sqrt{a^2 - \xi^2}}{C_2(x^2 + y^2 - \xi^2)^2 + 4x^2y^2} \left[x(x^2 + y^2 - \xi^2)\sqrt{C_2 - C_1} \right. \\ &\left. - y(x^2 + y^2 + \xi^2)\sqrt{C_2 - C_1} \right] \end{aligned}$$

$$C_1 = \frac{1}{2}(a^2 + y^2 - x^2); \quad C_2 = \sqrt{C_1^2 + x^2 y^2};$$

$$\Gamma = \left(\frac{1-\nu}{1+\nu} \right) \left[\frac{1}{(\xi-x_0)^2 + y_0^2} + \frac{1}{(\xi+x_0)^2 + y_0^2} \right] + 2y_0^2 \left\{ \left[\frac{1}{(\xi-x_0)^2 + y_0^2} \right]^2 + \left[\frac{1}{(\xi+x_0)^2 + y_0^2} \right]^2 \right\}$$

Setting the point force Q equal to unity, the influence coefficients A_{ij}^s can be obtained from the equation (6):

$$\nu = \frac{Q(1+\nu)}{4\pi E t_s} \left\{ \left[(3-\nu) \left(\ln \frac{d}{4y_0} - 1 \right) + 1 + \nu \right] + 2 \sum_{n=1}^{\infty} \left[(3-\nu) \ln \frac{nw}{\sqrt{n^2 w^2 + 4y_0^2}} + \frac{4y_0^2(1+\nu)}{n^2 w^2 + 4y_0^2} \right] \right\} \quad (6)$$

Once, all influence coefficients are determined we obtain a closed system of algebraic equations from which the unknown forces Q_1, Q_2 , can be calculated numerically. The Fig. 8 illustrates the convergence of the computational procedure.

The obtained forces contribute additional traction to the piecewise traction distribution $p(x)$ originally shown in Fig. 4b affecting the structural integrity of the reinforced structure in a positive way, and as such improving the failure control and overall survivability of the spacecraft.

4. MODEL VALIDATION

This section gives the numerical examples which illustrate the application of the method of singular integral equations for the structures with cracks or crack-like damages.

The Fig. 9 illustrates the evolution of the crack tip opening displacement after an impact hole was suddenly introduced in the loaded plate made of

aluminum alloy 2024. It is known that the ratio of the radial crack length ($L_{rad.cr.}$) to the hole diameter (D_{hole}) has a considerable effect on the critical stress. Fig. 10 illustrates that the singular integral equations method allows obtaining the accurate result for any specific case of ($L_{rad.cr.}/D_{hole}$)-ratio. The obtained results also illustrate the fact that for $L_{rad.cr.}/D_{hole} > 0.25$, the hole with two radial cracks can be considered as a straight crack.

In order to verify above method and illustrate its application, numerical calculations were performed and compared with results of impact and tensile tests of the 3-mm thickness specimens fabricated from alloy 2024. The computational analysis predicted residual strength to within 5% of the experimental data given in [4].

The validity of the present approach has been proved by comparing with the computational results obtained by the finite element method [1] to quantify the critical crack length in the cylindrical pressurized module experiencing 68.6 MPa hoop and 34.3 MPa longitudinal stresses respectively. The numerical analysis was performed for 2219-T87 aluminum alloy shell with the following parameters: $\sigma_u = 430$ MPa, $\sigma_y = 343$ MPa, $E = 73800$ MPa, $\nu = 0.33$, wall thickness $t_s = 3.17$ mm, toughness at the crack initiation $K_{Ic} = 68$ MPa·m^{1/2} and toughness at the maximum load $K_{Ic max} = 92$ MPa·m^{1/2} [1]

The comparisons presented in Table 1 shows that the computational results obtained by the finite element and singular integral equations methods are in fair agreement.

The numerical experiments on the reinforced habitable modules of the International Space Station showed the “unzipping” of the pressure wall is unlikely.

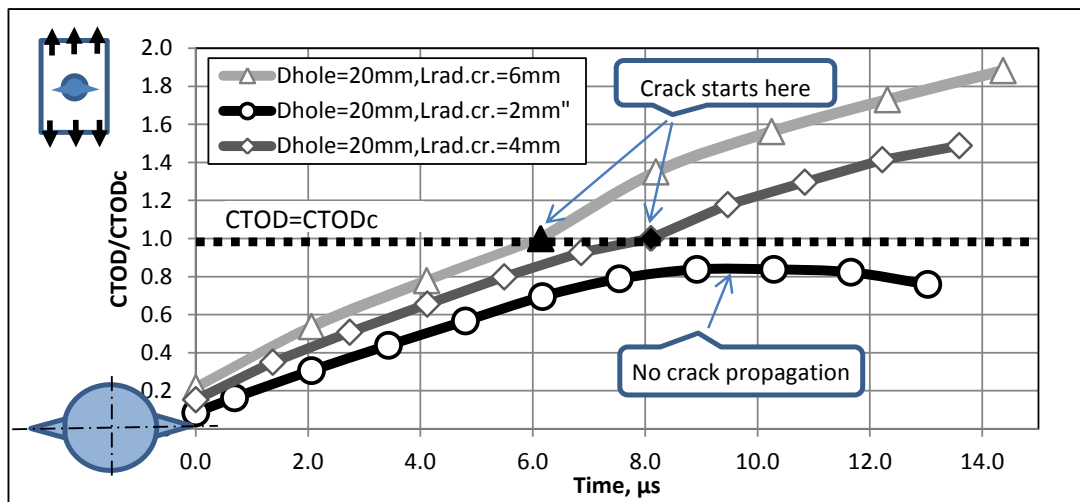


Fig. 9. Evolution of the crack tip opening displacement

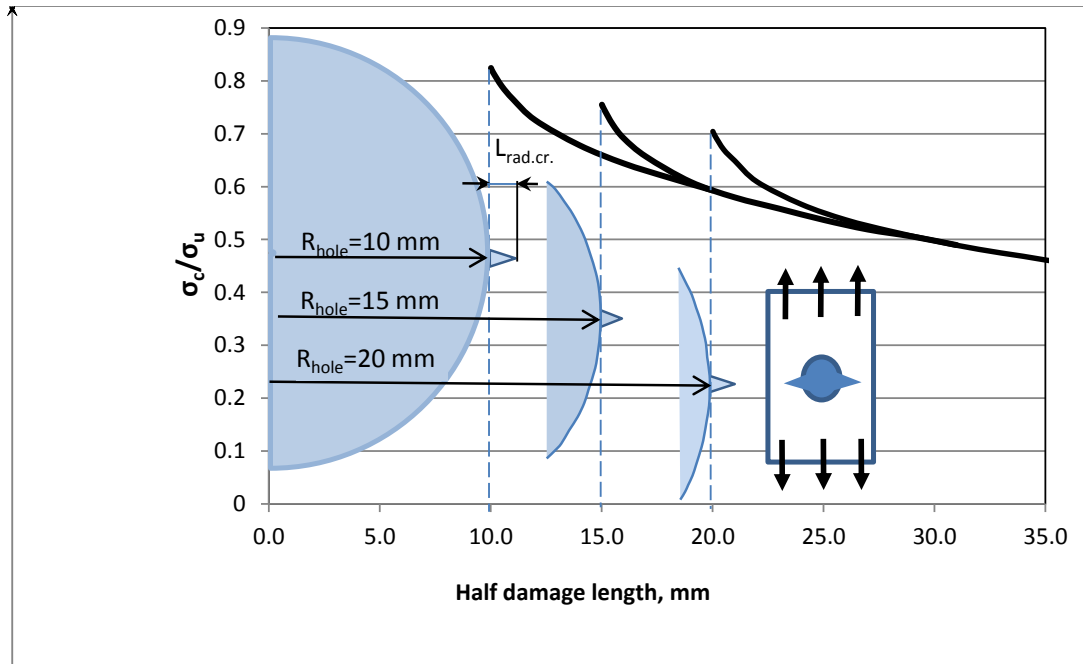


Fig. 10. Critical stress for various $(L_{rad.cr}/D_{hole})$ -ratio

Method	Critical crack length, mm	
	Crack initiation	Crack unstable
Elasto-	<599	1041
Present	590	1082
Deviation,%	N/A	3.4

Table 1. Critical crack length (specimen: 2219-T87, $t_s=3.17$ mm)

5. CONCLUSIONS

The present paper is focused on the engineering methodology which is viewed as a key element in the spacecraft design procedure providing that under no circumstances will the “unzipping” occur. A model of crack propagation in impact-damaged pressurized aerospace structure is presented. The numerical solution is obtained by the method of mechanical quadratures. Comparisons of the calculated results with the test data and numerical results obtained by finite element method showed good agreement. Therefore, the suggested SIE-based approach is concluded to be effective way of assessing the fracture behavior of the impact damaged aerospace pressurized structures.

6. ACKNOWLEDGEMENTS

The author would like to acknowledge the support of the Natural Sciences and Engineering Research Council of Canada (NSERC) under Discovery Grant.

7. REFERENCES

- Couque, H et al (1993). SwRI-NASA CR 64-00133.
- Lutz, B.E. & Goodwin, C. J. (1996). NASA CR 4720.
- Elfer, N. C. (1996) NASA CR 4706.
- Telichev, I. (2011) Unstable crack propagation in spacecraft pressurized structure subjected to orbital debris impact. *Canadian Aeronautics and Space Journal*; **57**(1), 106-111.
- Savruk, M. P. (2004) Method of singular integral equations in linear and elastoplastic problems of fracture mechanics. *Mat. Sci.*; **40**(3), 337-351.
- Telichev, I., Cook, F. (2012) Model of crack propagation in impact-damaged pressurized aerospace structure. *In Proc. CSME Int. Congress*, (CD-ROM), Winnipeg, Canada.
- Handbook for Damage Tolerant Design (2013), US AFRL/VASM, , Air Force Aircraft Structural Integrity Program, Online handbook.
- Poe, C. C. Stress-intensity factor for a cracked sheet with riveted and uniformly spaced stringers, NASA TR R-358, 1971.
- Westergaard, H. M. (1939) Bearing Pressures and Cracks. *J. Appl. Mech.*, **6**(2), A-49 - A-53.